RSC Advances

ROYAL SOCIETY
OF CHEMISTRY

www.rsc.org/advances

Simulation and Optimization of Horizontal Ammonia Synthesis Reactor Using Genetic Algorithm

M.J. Azarhoosh[a*], F. Farivar[a], and H. Ale Ebrahim[a]

[a] Chemical Engineering Department, Petrochemical Center of Excellence, Amirkabir University of

Technology (Tehran Polytechnic), Tehran 15875-4413, Iran

Abstract

Synthesis of ammonia from nitrogen and hydrogen is one of the most important processes in the petrochemical industry. In this study simulation and optimization of horizontal ammonia synthesis reactor was presented in two cases: first, intercooled horizontal ammonia synthesis reactor of the Khorasan petrochemical plant, second, horizontal ammonia synthesis reactor with two quench flows. The one dimensional heterogeneous mathematical model consists of two point boundary value differential equations for the catalyst pellets were used in the simulations. Also, effectiveness factor was calculated by both empirical relation and considering the diffusion-reaction equations. The differential equations of boundary and initial value problems were solved with combination of Runge-Kutta method and an improved shooting method. Simulation has been done in two cases. The first case is an intercooled horizontal ammonia converter. Also, the second case is a horizontal ammonia converter with two quench flows. Good agreements have been achieved between simulated results, .i.e., outlet component mole fraction and temperature, and industrial data (Khorasan plant data and SRI report). Then effect of parameters like inlet temperature, total feed flow rate, and operating pressure on ammonia production was studied. Finally, optimum solutions for the maximum mass flow rate production of ammonia were determined by Genetic Algorithm (GA). The adjustable parameters are inlet temperature, total feed flow rate and operating pressure. Results of optimization showed that maximum ammonia mass flux of 52433 kg/h and 73979 kg/h was produced in both cases respectively, in which inlet temperature, feed flow rate, and operating pressure were $524\,°C$, 217005 kg/h and 167 atm in the first case and 437 $°C$, 354986 kg/h and 237 atm in the second.

[*]Corresponding author. Tel.: +98 9387295609. fax: +98 66405847 E-mail address: m.j.azarhoosh@aut.ac.ir .

Keywords: Simulation, Optimization, Horizontal reactor, Ammonia synthesis, Genetic Algorithm

1. Introduction

Ammonia is one of the most important petrochemical products that are being manufactured worldwide. The largest fraction of ammonia is used for production of fertilizers like ammonium nitrate, ammonium phosphate, and urea [1]. Moreover, ammonia is an essential material for producing other chemicals such as nitric acid, ethanol amines, and toluene diisocyanate.

Ammonia synthesis reactor is the heart of an ammonia production plant. Numerous researches on the mathematical modeling of ammonia synthesis reactor have been done [2-7]. Many of these studies have shown that mathematical modeling is a convenient way to analyze and optimization of the reactor [6-11]. In practice, a small improvement in conversion degree considerably affects the overall economic balance of the ammonia production plant. Therefore, accurate modeling is essential for analysis and design.

Ammonia synthesis is a straightforward reaction and there is no side reaction. Synthesis reaction based on the Haber-Bosh process takes place at high temperatures and pressures over a magnetic iron oxide or, recently Ru based catalysts [12]. These reactors require a cooling system to achieve a high degree of conversion, because the reaction is highly exothermic. Based on the implemented cooling method, there are two types of converters for ammonia synthesis; tube-cooled converters, and quench type converters [13].

Many studies on the modeling and simulation of various configurations for ammonia converter have been carried out. Annable is among the first researchers who studied the modeling of steady state ammonia converters [14]. Baddour et al. developed a simple pseudo-homogeneous steady state model for Tennessee Valley Authority (TVA) type converters [15]. Panahande et al. developed a two dimensional model for the axial-radial ammonia synthesis reactor [16]. None of the above mentioned studies are about the horizontal ammonia converter. Dashti et al. recently simulated a horizontal ammonia converter with an internal heat exchanger [17]. Density and viscosity have been assumed constant in the modeling;

however, since temperature and pressure varies along the converter, density and viscosity of the gas mixture will change to a certain extent.

There are very few references use Evolutionary Algorithm (EA) techniques in chemistry and catalysis includes Genetic Algorithm (GA), Evolutionary Strategy (ES), Genetic programming (GP), etc. Evolutionary Strategy (ES) was used for selection and optimization of heterogeneous catalytic materials [18]. Genetic Programming has been employed very few. Baumes et al. [19, 20] showed two examples of this very powerful technique. Genetic Algorithms (GA) have been done by various groups such as Pereira el al. [21] study. They reported a study of the effect of Genetic Algorithm (GA) configurations on the performance of heterogeneous catalyst optimization. Also, Gobin et al. [22, 23] used multi-objective experimental design of experiments based on a genetic algorithm to optimize the combinations and concentrations of solid catalyst systems. Moreover, genetic algorithm merges with knowledge based system [24] and has been boosted on a GPU hardware to solve a zeolite structure [25, 26]. In addition, GA has been used for crystallography and XRD measurements [27, 28] and as an Active Learning method for effective sampling [29].

Although a number of papers on production of ammonia are available, very few have tried to optimize the process conditions to get the maximum benefit. In this study, an improved model for horizontal ammonia synthesis reactor was developed in two cases. First, the intercooled horizontal ammonia synthesis reactor of the Khorasan petrochemical plant, and second, the horizontal ammonia synthesis reactor with two quench flows. The effect of density and viscosity change as well as pressure change along the bed length was considered in the model. Furthermore, heat capacity of species was considered as a variable along the beds in order to increase accuracy. The effectiveness factor was calculated by both an empirical relation and a diffusion-reaction approach. The fourth-order Runge-Kutta method was used to solve the set of differential equations of the boundary and initial value problems. The modeling results were compared with some industrial data with a good agreement. Then the effect of parameters like inlet temperature, pressure, and total mass flow rate on conversion was studied. Finally, optimum conditions for the

maximum mass flow rate production of ammonia were determined by the Genetic Algorithm (GA). The adjustable parameters were inlet temperature, total feed flow rate, and operating pressure.

2. Horizontal converter description

Compared to the vertical converters a horizontal converter containing three adiabatic catalytic beds has the characters of a larger flow cross section and a shorter flow length. On the other hand small catalyst particles can be used to increase internal surface, the macro reaction rate and the outlet ammonia concentration [30]. Therefore the horizontal configuration overcomes some disadvantages of the vertical converters such as high pressure drop, large vessel diameter, and high catalyst volume [31]. Furtheremore the catalyst bed is arranged in a basket that fits into a horizontal shell, so that catalyst loading and unloading is facilitated [30]. This design has been developed by M.W. Kellogg, and it has been proven to be economical to use in industry [31]. There are different types of such converters with various cooling methods and a different number of beds [32-34].

2.1. First case

Figure 1 shows the overall layout of an intercooled horizontal ammonia converter. The feed, after entering the reactor, passes through the shell of the internal heat exchanger where its temperature raises. When the gas passes the first bed and the reaction takes place, its temperature increases and then enters the tubes of the heat exchanger to cool down. No specific operation is carried out between the second and third bed.
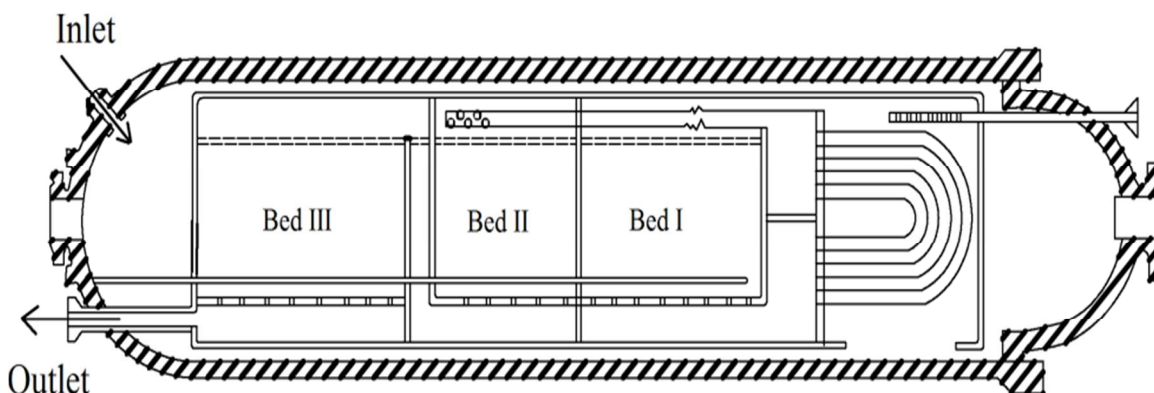
Fig.1. Horizontal intercooled ammonia converter

2.2. Second case

The horizontal ammonia converter with two quench flows is illustrated in figure 2. The reactor inlet gas is divided to three parts: mainstream, first quench flow, and second quench flow. The mainstream passes through an empty space of beds and the reactor wall and goes to the internal heat exchanger where it is heated with the output product stream. In the heat exchanger, the gas preheats to about 400 °C and then it enters the first bed. After passing through the first bed, temperature is increased to about 496 °C. The output gas from the first bed is quenched with the first quench flow and consequently its temperature is decreased. After that, it is sent into the second bed. Similarly, the output gas from the second bed is mixed with the second quench flow and is entered to the third bed. Finally, the product gas from the third bed is directed out of the converter through the heat exchanger.
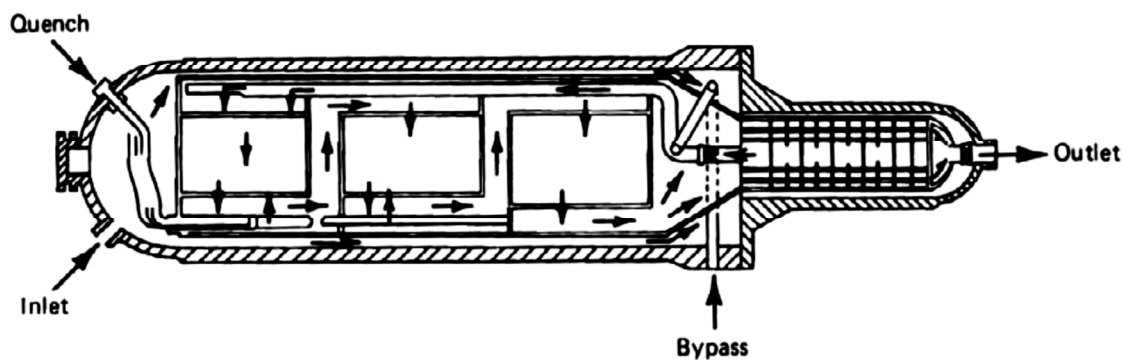
Fig.2. Horizontal ammonia converter with two quench flows [34]

3. Mathematical model

The following assumptions have been considered in the mathematical modeling:

   1- The model is heterogeneous and one dimensional.

   2- Heat and mass dispersions in the longitudinal direction are negligible [6].

3- The reactor is operating at steady-state condition.

4- The heat transfer resistance between the pellets and gas is negligible [6].

3.1. Mass balance (bulk gas)

In molar differential balance, nitrogen considered as a reference component gives mass balance equation as:

$$\frac{dX_{N_2}}{dl} = \frac{\eta R_{NH_3} A}{2 F_{N_2}{}^0} \tag{1}$$

3.2. Reaction rate

The modified Temkin equation was used to calculate the intrinsic rate of the reaction as follows [35]:

$$R_{NH_3} = k_2 \left[K_a{}^2 a_{N_2} \left(\frac{a_{H_2}{}^3}{a_{NH_3}{}^2} \right)^{\alpha} - \left(\frac{a_{NH_3}{}^2}{a_{H_2}{}^3} \right)^{1-\alpha} \right] \tag{2}$$

α is a constant between 0.5 to 0.75 [35]. In this work, $\alpha = 0.5$ was used. K_a was calculated as follows [6]:

$$\log_{10} K_a = -2.691122 \log T - 5.519265 \times 10^{-5} T + 1.848863 \times 10^{-7} T^2 + \frac{2001.6}{T} + 2.6899 \tag{3}$$

In equation (3), T represents the temperature in kelvin. k_2 was estimated by an Arrhenius relation as follows [7]:

$$k_2 = 1.7698 \times 10^{15} e^{-\left(\frac{E_2}{R_g T} \right)} \tag{4}$$

Where, $E_2 = 4.184 \times \frac{(40765) kJ}{kmol}$ is activation energy [35].

The components activity can be defined as:

$$a_i = \frac{f_i}{f_i^0} \tag{5}$$

Where, f_i^0 is reference fugacity and was assumed to be 101.325 kPa. Hence:

$$a_i = f_i = y_i \phi_i P \tag{6}$$

The fugacity coefficients of nitrogen, hydrogen, and ammonia can be determined from [35] (Table 1):

Table 1. Fugacity coefficients of nitrogen, hydrogen and ammonia [35]

$$\phi_{N_2} = 0.93431737 + 0.3101804 \times 10^{-3}T + 0.295896 \times 10^{-3}P - 0.2707279 \times 10^{-6}T^2 + 0.477507 \times 10^{-6}P^2 \tag{7}$$

$$\phi_{H_2} = e^{\left[e^{\left(-8.8402T^{0.125}+0.541 \right)}P - e^{\left(-0.1263T^{0.5}-15.980 \right)}P^2 + 300e^{\left(-0.011901T-5.941 \right)}\left(e^{\frac{-P}{300}}-1 \right) \right]} \tag{8}$$

$$\phi_{NH_3} = 0.1438996 + 0.2028538 \times 10^{-2}T - 0.448762 \times 10^{-3}P - 0.1142945 \times 10^{-5}T^2 + 0.2761216 \times 10^{-6}P \tag{9}$$

3.3. Energy balance

Using the energy balance for a differential element in the catalyst bed of the converter yields:

$$\dot{m}C_{p_{mix}} \frac{dT}{dl} = -\Delta H_r A \eta R_{NH_3} \tag{10}$$

$C_{p_{mix}}$ is specific heat for the gas mixture. Specific heat for pure components is a function of temperature

and pressure that is given in Table 2 [11]:

Table 2. Specific heats for pure components [11]

$$\left(C_p\right)_{H_2} = 4.184\left(6.952 - 0.04576 \times 10^{-2}T + 0.09563 \times 10^{-5}T^2 - 0.2079 \times 10^{-9}T^3\right) \tag{11}$$

$$\left(C_p\right)_{N_2} = 4.184\left(6.903 - 0.03753 \times 10^{-2}T + 0.1930 \times 10^{-5}T^2 - 0.6861 \times 10^{-9}T^3\right) \tag{12}$$

$$\left(C_p\right)_{NH_3} = 4.184(6.5846 - 0.61251 \times 10^{-2}T + 0.23663 \times 10^{-5}T^2 - 1.5981 \times 10^{-9}T^3 + [96.1778 -$$
$$0.067571P + (-0.2225 + 1.6847 \times 10^{-4}P)T + (1.289 \times 10^{-4} - 1.0095 \times 10^{-7}P)T^2]) \tag{13}$$

$$\left(C_p\right)_{CH_4} = 4.184\left(4.750 + 1.200 \times 10^{-2}T + 0.3030 \times 10^{-5}T^2 - 2.630 \times 10^{-9}T^3\right) \tag{14}$$

$$\left(C_p\right)_{N_2} = 4.184(4.9675) \tag{15}$$

It must be mentioned that the average specific heat of the reaction varies with degree of conversion. Here, the heat of reaction was calculated from the following equation [36]:

$$\Delta H_r = 9723.24[-23840.57 + (P - 300.0)(1.08 + (P - 300.0)(0.01305 + (P - 300.0)(0.83502$$
$$\times 10^5 + (P - 300.0) \times 0.65934 \times 10^{-7}))) + 4.5 \times (1391.0 - T) \tag{16}$$

3.4. Pressure drop

The pressure drop along the catalyst beds of the converter has been calculated by Ergun equation for one dimensional flow as follows [37]:

$$\Delta P = -\mu \nabla^2 u = -\frac{150(1-\varepsilon)^2}{\varepsilon^3}\left(\frac{\mu u}{d_P^2}\right) = 1.75\frac{1-\varepsilon}{\varepsilon^3}\left(\frac{\rho u^2}{d_P}\right) \tag{17}$$

The density of the gas mixtures has been calculated by modification of the perfect gas law as follows [38]:

$$\rho = \frac{PM_{av}}{ZR_gT} \tag{18}$$

Viscosity of the components was accurately corrected as a function of temperature [38]:

$$\mu = \frac{AT^B}{1 + \dfrac{C}{T} + \dfrac{D}{T^2}} \tag{19}$$

In which, A, B, C, and D, constants are available for about 1500 components in the reference [39]. In order to predict the viscosity of gaseous mixtures, the Bromley and Wilke method was used [37]. Here, the Stiel and Thodos method was used in order to correct it at high pressures [38].

3.5. Effectiveness factor (η)

In this work, the effectiveness factor has been calculated by two approaches, an empirical relation and also the diffusion-reaction model approach [40]. Simulation results for both methods have been compared along the reactor beds.

3.5.1. The empirical relation

The empirical relation for the effectiveness factor with respect to temperature and conversion has been developed by Dyson and Simon as follows [35]:

$$\eta = b_0 + b_1T + b_2X + b_3T^2 + b_4X^2 + b_5T^3 + b_6X^3 \tag{20}$$

In the above equation, X is the conversion of nitrogen, and b_i are coefficients where their values for different operating pressures were presented in reference [35]. In this work, coefficients for 15000 kPa were used. The coefficients for this pressure are given in Table 3.

Table 3. Coefficients of empirical relation (20) for effectiveness factor calculation [35]

b_0	b_1	b_2	$b_3 \times 10^4$	b_4	$b_5 \times 10^8$	b_6
-17.539096	0.07696844	6.900548	-1.08279	-26.4247	4.92765	38.9373

3.5.2. Diffusion and reaction approach

In this approach, the diffusion through the catalyst pores was considered by a molar differential balance for component i inside the catalyst particle:

$$\frac{1}{r^2}\frac{d}{dr}\left(r^2 N_i\right) = \gamma_i \frac{R_{NH_3}(X,T,P)}{1-\varepsilon} \tag{21}$$

Where γ_i is stoichiometric coefficient of the i'th component. After some straightforward manipulations, the equation will have the following dimensionless form [6]:

$$\frac{d^2 y_i}{dw^2} - \frac{1}{\gamma_i + y_i}\left(\frac{dy_i}{dw}\right)^2 + \frac{2}{w}\frac{dy_i}{dw} = -\left(\frac{R_P^2}{CD_{i,e}}\right)(\gamma_i + y_i)\frac{R_{NH_3}(y,T,P)}{1-\varepsilon} \tag{22}$$

The boundary conditions are:

$$w = 0 \qquad \frac{dy_i}{dw} = 0$$

$$w = 1 \qquad y_i = y_{ig}$$

Where $w = \dfrac{r}{R_P}$, and C is the total concentration that is defined as:

10

$$C = \frac{\sum_{i=1}^{n} f_i}{R_g T} \qquad (23)$$

The effective diffusion coefficients are calculated with the relation given by Elnashaie and Elshishini [40]:

$$D_{ie} = \frac{1}{2} \theta D_i \qquad (24)$$

The Stefan-Maxwell equation for multi-component diffusion was used for computing the diffusion coefficients of components [6]:

$$D_i^\circ = \frac{1}{\sum_{j=1, j\neq i}^{n} \left(\frac{1}{D_{ji}^\circ} \right) \left(y_{jb} - Z_j y_{ig} \frac{Z_j}{Z_i} \right)} \qquad (25)$$

Where

$$Z_i = \frac{N_i}{N_1 + N_2 + N_3}; i = 1,2,3 \qquad (26)$$

After calculation of the intraparticle concentration from equation (22), the effectiveness factor can be computed as [41]:

$$\eta = \frac{\int_0^{R_P} r^2 R_{NH_3} \left(y_{NH_3}^s, T \right)}{R_{NH_3, s} \int_0^{R_P} r^2 dr} \qquad (27)$$

4. Numerical solution algorithm

The first step to solve the model equations is to calculate the effectiveness factor at the entrance of the reactor. In the diffusion-reaction approach, the effectiveness factor can be obtained by solving the catalyst

11

pellet equations. These equations are non-linear boundary value problems. There are several methods for solving equation (22). The finite difference and orthogonal collocation methods convert the problem to a set of algebraic equations. When equation (22) is nonlinear, the resulting set of equations is also nonlinear. The solution of the nonlinear equations may not be unique and the generation of any solution may be difficult [42]. Combination of fourth-order Runge-Kutta method with an improved shooting method was used to solve these set of differential equations [42]. The conventional shooting method converts the boundary value problem into an initial value problem. Starting with an assumed condition for the missing initial condition and improving it through iteration, the method tries to reach a solution that agrees with all the given boundary conditions. In the conventional forward shooting, integration of Eq. (22) starts at $w = 0$ with $\frac{dy_i}{dw} = 0$ and an assumed $y_i(0)$, the missing part in the problem. Unless the computed $y_i(1)$ with Runge-Kutta method agrees with the boundary condition of $y_i(1) = y_{ig}$, $y_i(0)$ is adjusted in an iterative procedure until the assumed $y_i(0)$ yields a solution that agrees with the boundary condition within a specified tolerance. The conventional shooting method can be applied to compute the effectiveness factors only when the concentration at the catalyst center is greater than zero, i.e., $y_i(0) > 0$,because $y_i(0) = 0$ always results in a trivial solution $y_i(w) = 0$ in the method. Indeed, $y_i(0) = 0$ can occur when the reaction order is less than one and the Thiele modulus is large. To overcome such limitations of the conventional shooting method, an improved shooting method is used. In this method, the reaction rate $f(y_i)$ is approximated as a linear function of the concentration y_i in an interval of $y_i = 0$ and $y_i = \psi$, a sufficiently small number which set as 10^{-9}. This approximation prevented $y_i(0)$, however small, from becoming zero. The proposed shooting method with the approximation has been found to be robust and efficient in computing the effectiveness factors [42]. Having the effectiveness factor, bulk phase mass and heat balance differential equations can be solved. This procedure should be repeated for each differential step to obtain the temperature, bulk gas concentrations of ingredients, and pressure profiles along the reactor length.

5. Genetic Algorithm (GA) optimization

The Genetic Algorithm is an optimization tool based on Darwinian evolution [43]. Genetic Algorithms start with randomly chosen parent chromosomes from the search space to create a population. They work with the chromosome genotype. The population evolves towards better chromosomes by applying genetic operators which model genetic processes occurring in the nature selection, recombination and mutation. Selection compares chromosomes in the population and chooses them to take part in the reproduction process. Selection also occurs with a given probability on the basis of fitness function. Fitness functions play the role of an environment to distinguish between good and bad solutions. The recombination is carried out after finishing the selection process. It combines, with predefined probability, features of two selected parent chromosomes and forms similar children. After the recombination, the offspring undergoes mutation. Generally, mutation refers to the creation of a new chromosome from one and only one individual with predefined probability. After three operators are carried out, the offspring is inserted in the population, replacing the parent chromosomes, from which they were derived, and produces a new generation. This cycle is performed until the optimization criterion is met [44]. A maximum number of generations and/or a maximum number of generations without improvement of the best individual generally act as stopping criterions [43].

6. Simulation results and discussion

The simulation has been carried out using MATLAB software for two cases.

6.1. First case

The operating conditions and data used in the simulation of intercooled horizontal ammonia synthesis reactor are given in Table 4.

Table 4. Operating conditions and data used in the simulation (first case)

Reactor characteristics	
Reactor length:	21.45 (m)

Reactor diameter:	2.8 (m)		
	Bed I	Bed II	Bed III
Bed depth (m)	0.93	0.93	0.93

Operating conditions

Total feed flow rate:	189932.42 (kg/h)		
Inlet temperature:	533 (K)		
Operating pressure:	125.82 (atm)		
Feed compositions:	NH_3=0.0222	N_2=0.2297	H_2=0.6672
	Ar=0.0226	CH_4=0.0583	

Figs. 3 and 4 show the compositions mole fraction and temperature profile along the beds, respectively.
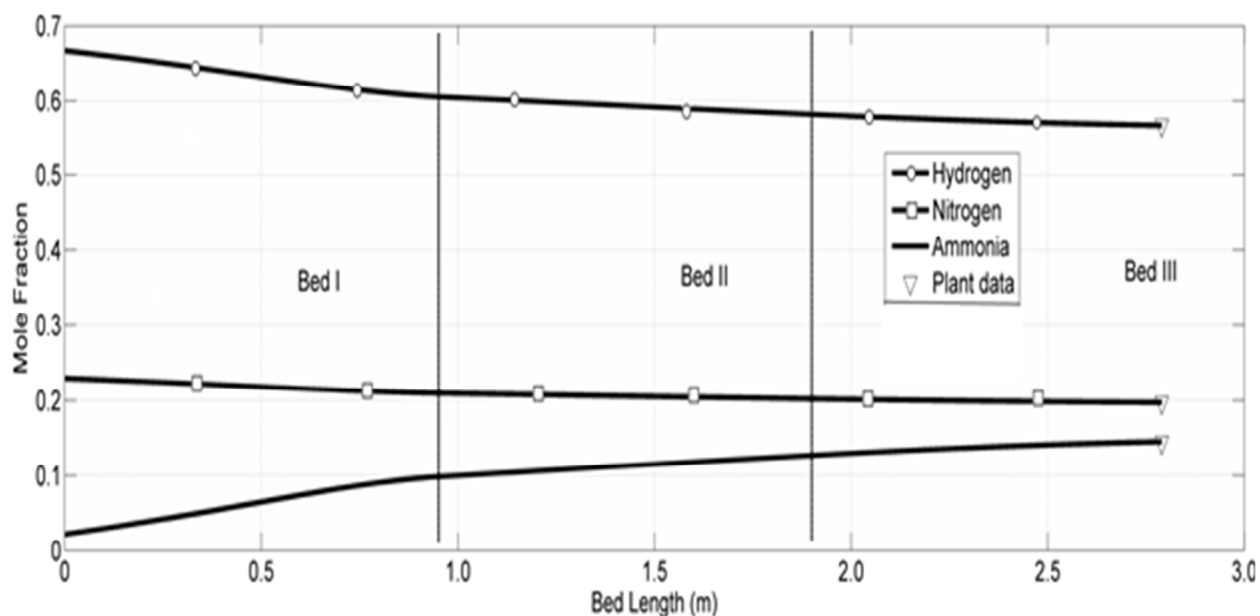
Fig.3. Mole fraction of component variation along the beds (first case)

14
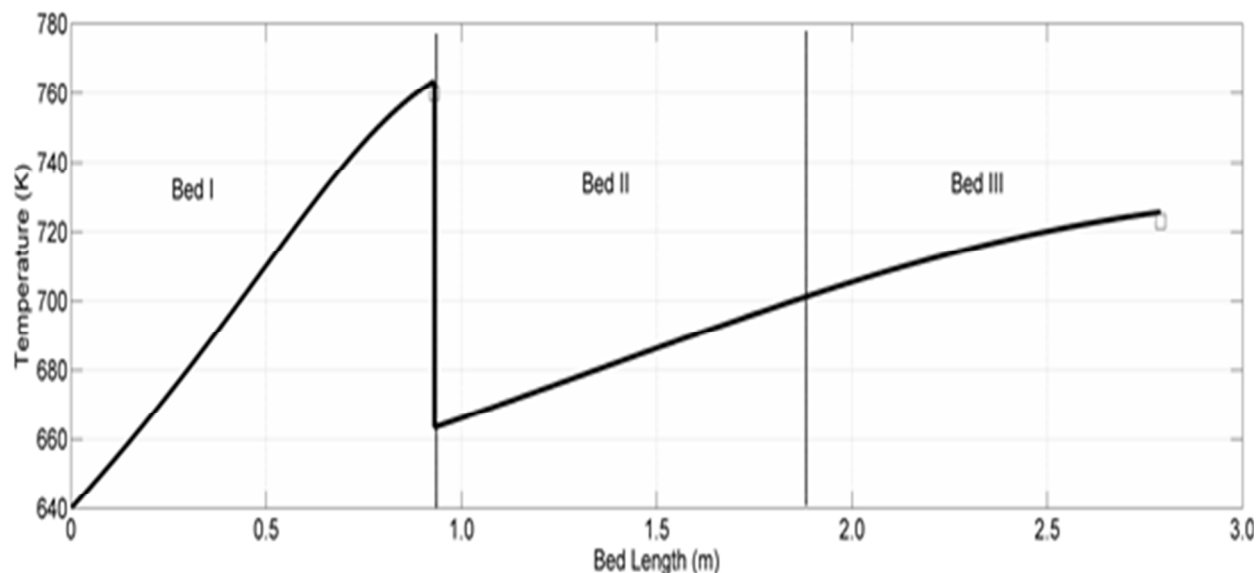
Fig.4. Temperature profile along the beds (first case)

The final results are summarized in Table 5. As it can be seen, good agreements have been achieved between simulated results and the Khorasan plant data.

Table 5. Simulation and industrial data for compositions mole fraction and temperature at reactor outlet (first case)

	Simulation	Plant data	Relative error (%)
Mole fraction			
Nitrogen	0.1976	0.1969	0.35
Hydrogen	0.5684	0.5679	0.09
Ammonia	0.1435	0.1442	0.48
Methane	0.0626	0.0655	4.43
Argon	0.0243	0.0255	4.70
Temperature (K)			
	725	723	0.27

Figure 5 shows conversion of nitrogen variation along the reactor beds.
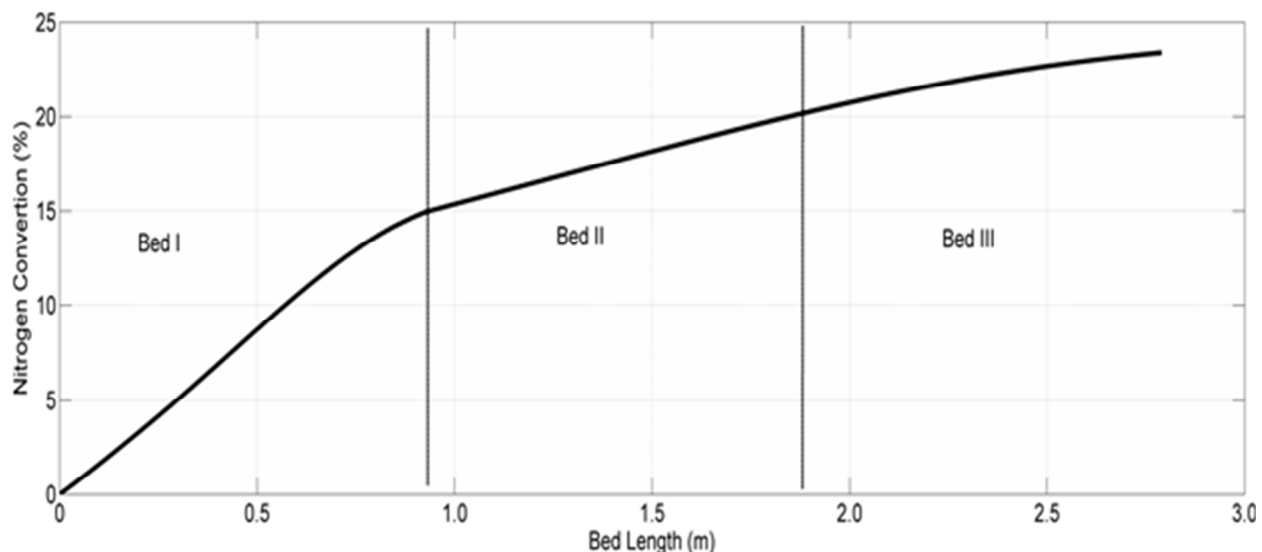
Fig.5. Nitrogen conversion profile along the reactor beds (first case)

The results confirm that the heterogeneous one dimensional model with variable density and viscosity shows a good accuracy and can be used for optimization or to study the effect of operating parameters on reactor performance.

6.2. Second case

The base case operating conditions and data used in the simulation for horizontal ammonia synthesis reactor with two quench flows are presented in Table 6.

Table 6. Operating conditions used for simulation of ammonia converter (second case) [45]

Nominal synthesis pressure (kPa)	20750
Input temperature (°C)	399
Total input feed flow rate (kg/h)	333703.58
Input compositions :	

16

NH_3	0.013
N_2	0.213
H_2	0.639
Ar	0.033
CH_4	0.102

Figure 6 shows the variation of the compositions along the beds. Black points in the figure represent the output industrial data [45]. The final results are summarized in Table 7. As it can be seen, good agreements have been achieved between simulated results and industrial data when the effectiveness factor is calculated by the diffusion-reaction approach.
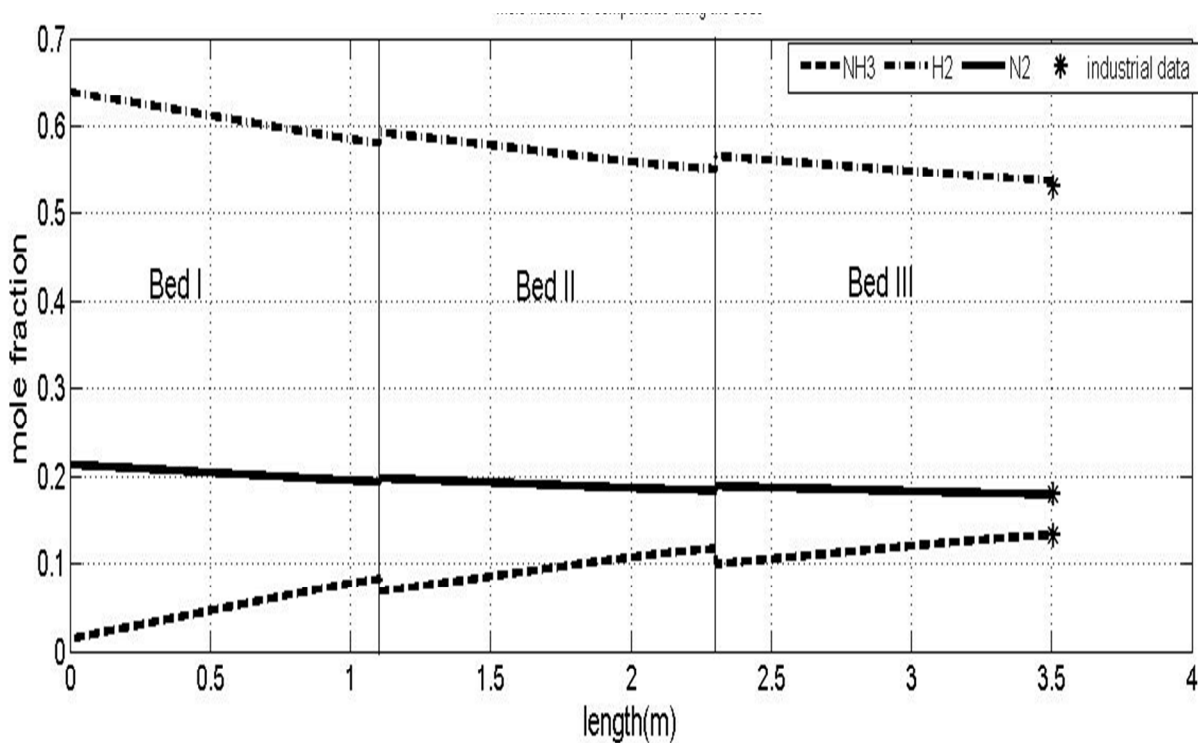
Fig.6. Compositions mole fraction profiles along the beds (second case)

Table 7. Simulation and industrial data for composition mole fraction at reactor outlet (second case) [45]

Composition	Simulation[1]	Simulation[2]	Industrial data	Relative Error (%)[1]	Relative Error (%)[1]
Nitrogen	0.182	0.180	0.179	1.68	0.56
Hydrogen	0.543	0.541	0.538	0.93	0.56
Ammonia	0.125	0.130	0.132	5.30	1.52
Methane	0.115	0.111	0.109	5.50	1.83
Argon	0.035	0.038	0.036	2.78	5.56

[1] empirical relation for effectiveness factor, [2] diffusion- reaction approach for effectiveness factor

Figures 7 and 8 show the conversion of N_2 and temperature change along the beds, respectively.
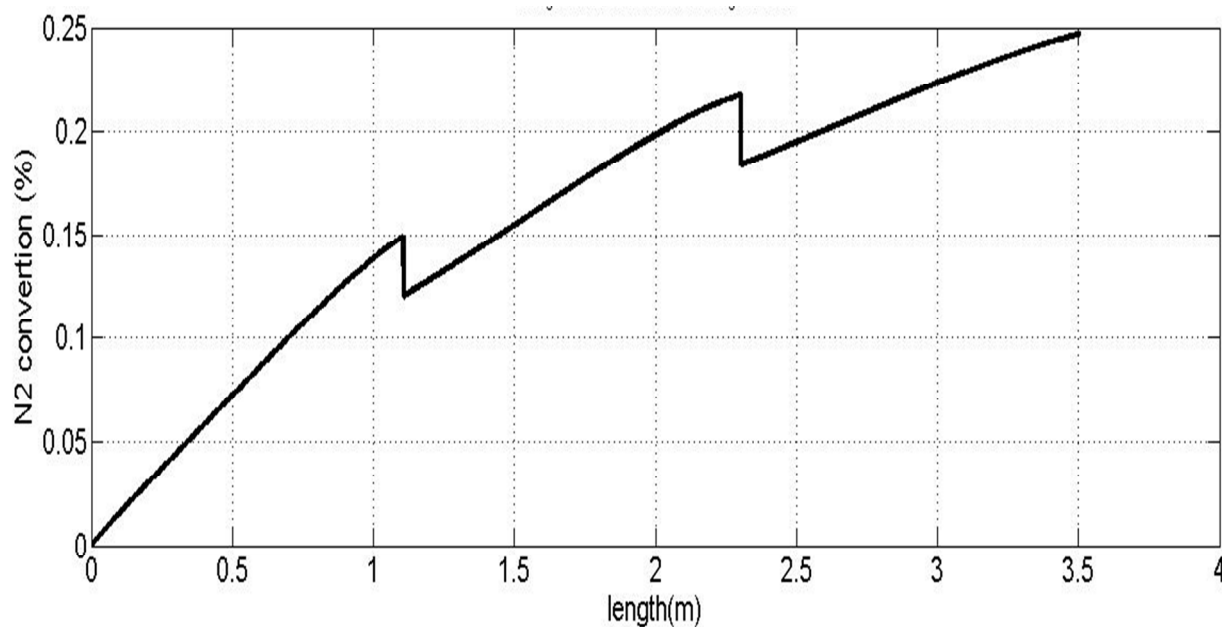
Fig.7. Profile of nitrogen conversion along the beds (second case)
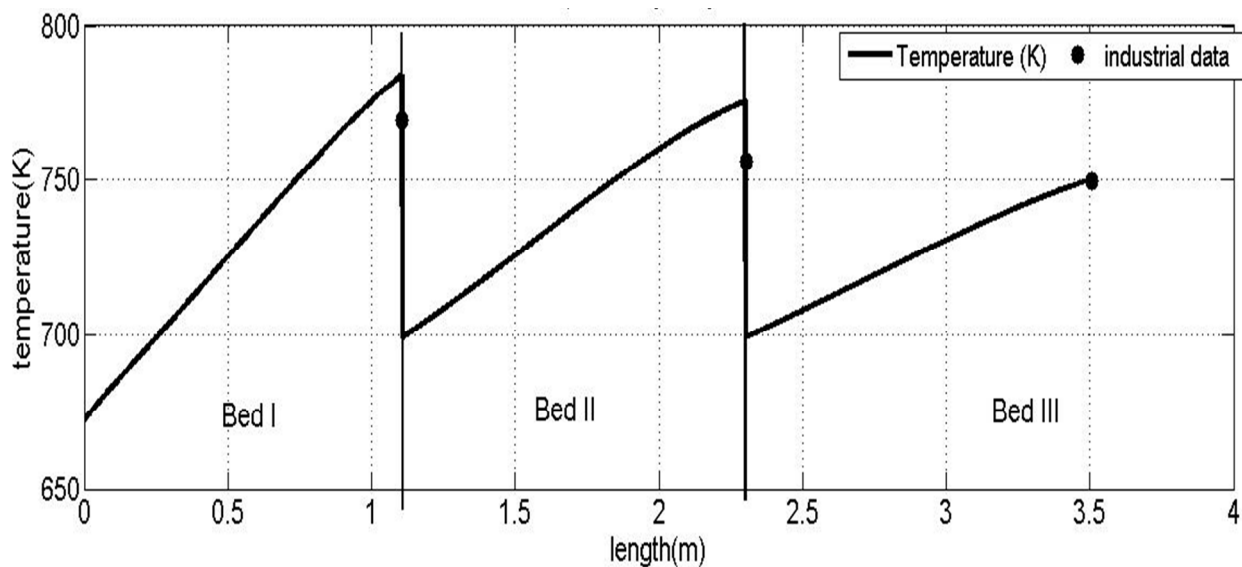
Fig.8. Temperature profile along the beds (second case)

In Table 8, the measured temperatures from the industrial plant are compared with simulation results.

Table 8. Simulation and industrial data [45] comparison for temperature (second case)

Bed no.	Industrial (K)	Simulation (K)	Error (relative)
I	770	781.3	1.46%
II	756	769.5	1.78%
III	750	751.4	0.18%

The results confirm that the heterogeneous one dimensional model with variable density and viscosity shows good accuracy.

Figs. 9 and 10 show the effectiveness factor profiles along the converter, calculated by the empirical relation and diffusion-reaction approach, respectively.
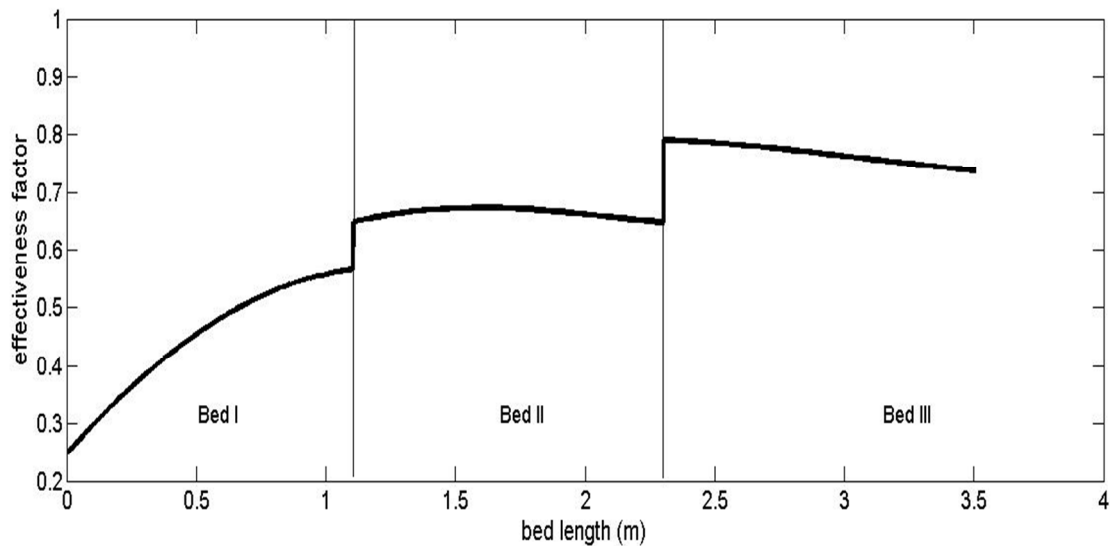
Fig.9. Effectiveness factor profile (empirical relation)
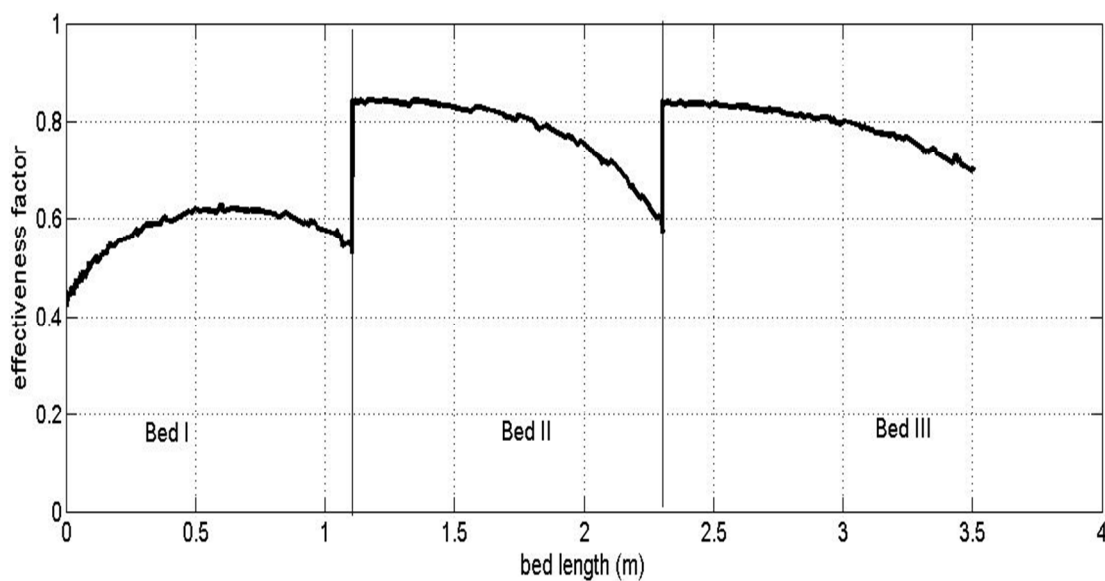
Fig.10. Effectiveness factor profile (diffusion-reaction approach)

The effectiveness factor is a measure of the effect of the diffusional limitations on the overall rate of reaction. As temperature increases along the reactor due to exothermic ammonia synthesis reaction, the rate constant and consequently Thiele modulus raise. Therefore, diffusional resistance increases, and a

decreasing trend is obtained for the effectiveness factor. In the cooling sections between the beds, the effectiveness factor jumps upward.

7. Analysis of effective parameters

In the following figures, the effect of variation in the inlet temperature, pressure, and flow rate on the nitrogen conversion has been investigated in the second case. Figure 11 shows the effect of inlet temperature on conversion of nitrogen for ammonia synthesis at 20750 kPa. According to this figure, as the inlet temperature increases, conversion usually increases at the end of the converter, but the slope of increase declines. For example, at a vessel pressure of 20750 kPa, up to 660 K, the conversion of nitrogen increases at the end of the converter. A further increase of inlet temperature will decrease the final conversion due to equilibrium constraint.

In Figure 12, the final conversions at different temperatures and pressures are shown. As it can be seen, for any given pressure, there is an optimal temperature in which the final conversion is maximum. Moreover, by increasing the pressure, the optimal temperature decreases.
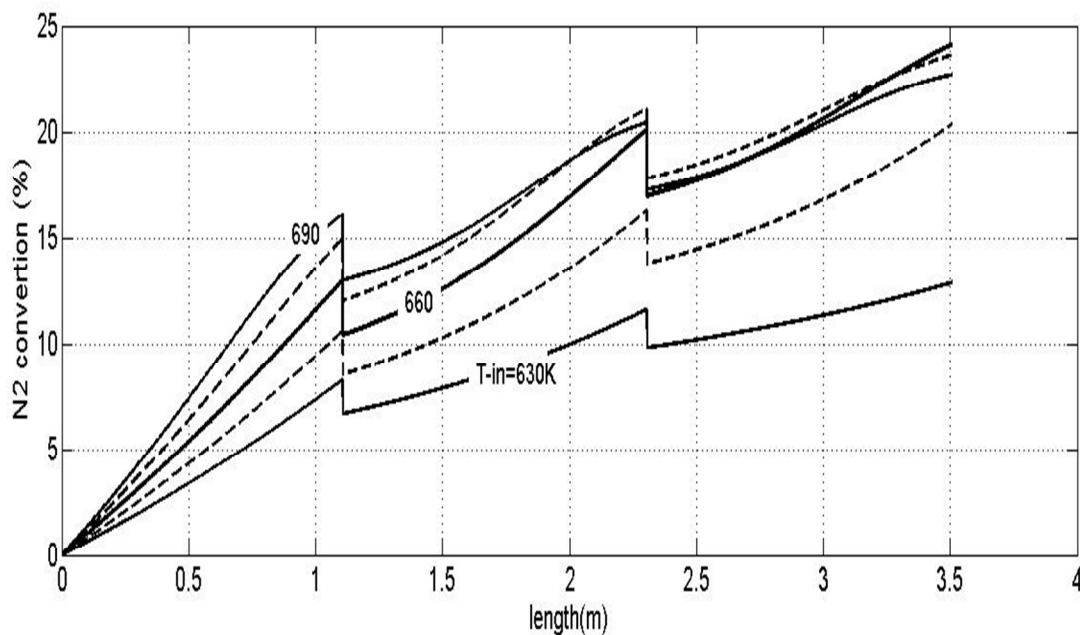
Fig.11. Conversion of N_2 along the beds at 20750 kPa in different inlet temperatures
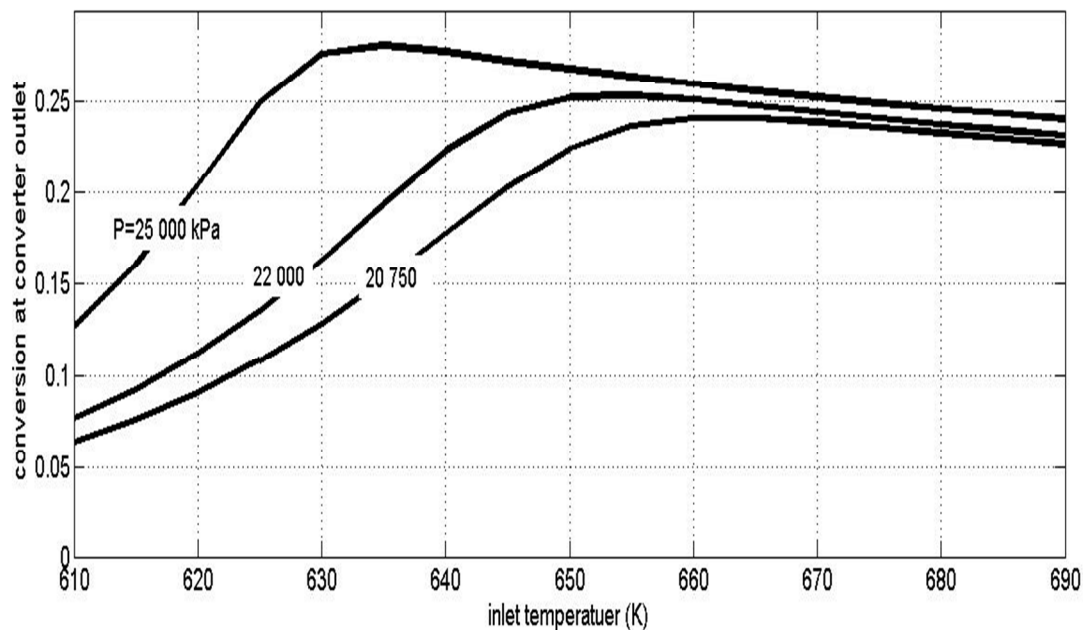
Fig.12. Final Conversion of N2 at different inlet pressures and temperatures

The product molar flow rate is a multiplication of the total feed flow rate and outlet mole fraction of ammonia. It is apparent that by increasing the total feed flow rate, the molar fraction of ammonia will decrease due to diminishing reactor residence time. However, the outlet ammonia flow rate has a maximum. Thus an optimum total feed flow rate with maximum ammonia production flow rate can be determined. In Figure 13, the effect of the total feed flow rate on the outlet ammonia molar flow rate is studied.
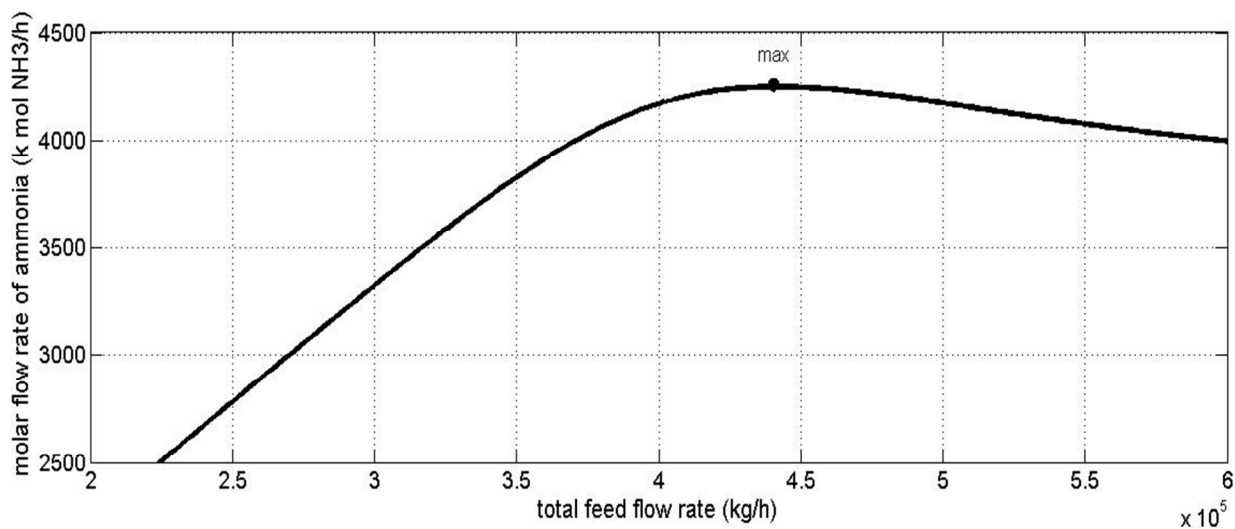
Fig.13. Effect of total feed flow rate on the produced ammonia flow rate in the converter

8. Optimization results and discussion

Single-objective Genetic Algorithm was used to optimize and obtain optimum solutions. A population size of 20 was chosen with crossover of 0.7 and mutation probability of 0.05. Input parameters of the Genetic Algorithm are given in Table 9.

Table 9. Input parameters of Genetic Algorithm

Parameter name	Method and value
Number of decision variables	3
Number of objectives	1
Population size	50
Crossover method	Arithmetic crossover
Crossover probability	0.7
Mutation method	Gaussian mutation
Mutation probability	0.05

The objective of optimization is maximum mass flow rate production of ammonia. The adjustable parameters are inlet temperature, total feed flow rate and operating pressure and their range is given in Table 10.

Table 10. Range of adjustable parameters

	First case	Second case
Inlet temperature	$400 \leq T_f \leq 600\,K$	$350 \leq T_f \leq 500\,K$
Total feed flow rate	$127500 \leq \dot{m}_i \leq 382500\,kg/h$	$300000 \leq \dot{m}_i \leq 400000\,kg/h$
operating pressure	$90 \leq P_i \leq 180\,atm$	$150 \leq P_i \leq 250\,atm$

Different operations were performed for 50 generations to obtain optimum solution. Table 11 shows the optimum solution.

Table 11. Results of optimization with genetic algorithm

	First case	Second case
Objective:		
maximum mass flow rate production of ammonia	$52433\,kg/h$	$73979\,kg/h$
Adjustable parameters :		
Inlet temperature	$524.4\,K$	$437.0\,K$
Total feed flow rate	$217005\,kg/h$	$354986\,kg/h$
operating pressure	$166.8\,atm$	$236.9\,atm$

Conclusions

In this work, the one dimensional heterogeneous mathematical model was applied for simulation of the horizontal ammonia synthesis reactors. The effectiveness factor was calculated by both empirical relations and the diffusion-reaction approach. Simulation has been done in two cases. The first case is an intercooled horizontal ammonia converter. Also, the second case is a horizontal ammonia converter with two quench flows. A good agreement between simulation predictions and some industrial data was achieved. Then the effect of variation in the inlet temperature, pressure, and flow rate on the nitrogen conversion has been investigated in the second case. As the inlet temperature increases, nitrogen conversion grows up at the end of the converter. Also, by increasing the total feed flow rate, the molar fraction of ammonia will decrease due to diminishing reactor residence time. However, the outlet ammonia flow rate has a maximum. Moreover, by increasing the pressure, the optimal temperature with maximum nitrogen conversion decreases. Finally, the best conditions for maximum mass flow rate production of ammonia were determined by Genetic Algorithm (GA) optimization. The adjustable parameters are inlet temperature, total feed flow rate, and operating pressure.

Acknowledgment

Nomenclature

$a_{H_2}, a_{NH_3}, a_{N_2}$	Activity of hydrogen, ammonia and nitrogen
A	Crosse section area of beds (m^2)
C	Total concentration (kmol/m^3)
$C_{p_{mix}}$	Specific heat of gas mixture (kJ/kg.K)
D_{ie}	Effective diffusion coefficient of component i (m^2/h)
f_i	Fugacity of component i (kPa)

f_i^0	Reference fugacity of component i (kPa)
$F_{N_2}^0$	Initial molar flow rate of nitrogen (kmol/h)
K_a	Equilibrium constant of reaction
k_2	Reverse reaction rate constant
l	Bed length (m)
$\dot{m}$	Mass flow rate (kg/h)
M_{av}	Average molecular weight (kmol/kg)
N_i	Molar flux of component i at catalyst particle (kmol/m^2.h)
P	Pressure [kPa]
r	Radial coordinate of catalyst particle (m)
R_g	Universal gas constant (kJ/kmol.K)
R_p	Equivalent radius of the catalyst particle (m)
R_{NH_3}	Intrinsic rate of reaction (kmol /m^3.h)
T	Temperature (K)
u	Velocity (m/h)
X	Conversion of nitrogen
y_i	Mole fraction of component i
y_i^s	Mole fraction of component i in catalyst particle

Greek Symbols

ε	Porosity of catalyst bed
η	Effectiveness factor

26

ϕ_i	Fugacity coefficient of component i
ΔH_r	Heat of reaction (kJ/kmol)
μ	fluid viscosity (Pa.s)
ρ	Density (kg/m^3)
θ	Intra-particle porosity

References:

[1] C.Y. Liu, Ph.D dissertation, Department of Environmental Chemistry and Engineering, Tokyo Institute of Technology, Tokyo, 2002.

[2] R. Angira, International Journal of Chemical Reactor Engineering, 2011, **9**, issue 1.

[3] M. T. Sadeghi and A. Kavianiboroujeni, International Journal of Chemical Reactor Engineering, 2008, **6**, issue 1.

[4] M.E.E. Abashar, Mathematical and computer modelling, 2003, **37**, 439.

[5] B.V. Babu and R. Angira, Computers & chemical engineering, 2005, **29**, 1041.

[6] S.S. Elnashaie, M.E. Abashar and A.S. Al-Ubaid, Industrial & Engineering Chemistry Research, 1988, **27**, 2015.

[7] Ch.P.P. Singh and D.N. Saraf, Industrial & Engineering Chemistry Process Design and Development, 1979, **18**, 364.

[8] M. De Tremblay and R. Luus, The Canadian Journal of Chemical Engineering, 1989, **67**, 494.

[9] S.S.E.H. Elnashaie, A.M. Adris, M.A. Soliman and A.S. Al-Ubaid, The Canadian Journal of Chemical Engineering, 1992, **70**, 786.

[10] F. Zardi, Modeling, Chemical Engineering Science, 1992, **47**, 2523.

[11] M. Shah, Industrial & Engineering Chemistry, 1967, **59**, 72.

[12] C.H. Bartholomew and R.J. Farrauto, Fundamentals of industrial catalytic processes, 2nd ed. Hoboken: Wiley and Sons, 2005.

[13] M. Appl, Ammonia: Principles and Industrial Practice, 1st ed, Hoboken: Wiley-VCH, 1999.

[14] D. Annable, Chemical Engineering Science, 1952, **1**, 145.

[15] R.F. Baddour, P.L.T. Brian, B.A. Logeais and J.P. Eymery, Chemical Engineering Science 1965, **20**, 281.

[16] M.R. Panahandeh, J. Fathikaljahi and M. Taheri, Chemical engineering & technology, 2003, **26**, 666.

[17] A. Dashti, K. Khorsand, M. Ahmadi Marvast and M. Kakavand, Petroleum and Coal, 2006, **48**, 15.

[18] D. Wolf, O.V. Buyevskaya and M. Baerns, Applied Catalysis A: General, 2000, **200**, 63.

[19] L.A. Baumes, A. Blansché, P. Serna, A. Tchougang, N. Lachiche, P. Collet and A. Corma, Materials and Manufacturing Processes, 2009, **24**, 282.

[20] L.A. Baumes and P. Collet, Computational Materials Science, 2009, **45**, 27.

[21] S.R.M. Pereira, F. Clerc, D. Farrusseng, J.C. van der Waal, T. Maschmeyer and C. Mirodatos, QSAR & Combinatorial Science, 2005, **24**, 45.

[22] O.C. Gobin, A. Martinez Joaristi and F. Schüth, Journal of Catalysis, 2007**, 252**, 205.

[23] O.C. Gobin and F. Schüth, Journal of Combinatorial Chemistry, 2008, **10**, 835.

[24] J. M. Serra, A. Corma, D. Farrusseng, L.A. Baumes, C. Mirodatos, C. Flego and C. Perego, Catalysis Today, 2003, **81**, 425.

[25] J. Jiang, J.L. Jorda, J. Yu, L.A. Baumes, E. Mugnaioli, J.M. Diaz-Cabanas, U Kolb and A. Corma, Science, 2011, **333**, 1131.

[26] A. Rimmel, F. Teytaud and T. Cazenave, Optimization of the Nested Monte-Carlo Algorithm on the Traveling Salesman Problem with Time Windows, in Applications of Evolutionary Computation, G. Goos, J. Hartmanis and J.v. Leeuwen, Editors. 2010, Springer. p. 501-511.

[27] L.A. Baumes, M. Moliner and A. Corma, Chemistry – A European Journal, 2009, **15**, 4258.

[28] L.A. Baumes, M. Moliner, N. Nicoloyannis and A. Corma, CrystEngComm, 2008, **10**, 1321.

[29] L.A. Baumes, Journal of Combinatorial Chemistry, 2006, **8**, 304.

[30] Q. Ye, W. Ying and D. Fang, Chinese Journal of Chemical Engineering,2001, **9**, 441.

[31] O.J. Quartulli and A. Wagner, Hydrocarbon Process, 1978, **57**, 115.

[32] K.L. Blanchard, Cold wall horizontal ammonia convertor, 2008, Google patents.

[33] G.A. Denavit, R. Finello and R.B. Peterson, Horizontal ammonia converter, 1984, Google Patents.

[34] G.F. Froment, K.B. Bischoff and J. De Wilde, Chemical Reactor Analysis and Design, 3rd ed, Hoboken: John Wiley & Sons, 2010.

[35] D.C. Dyson and J.M. Simon, Industrial & Engineering Chemistry Fundamentals, 1968, **7**, 605.

[36] L.D. Gaines, Industrial & Engineering Chemistry Process Design and Development, 1977, **16**, 381.

[37] S. Ergun and A.A. Orning, Industrial & Engineering Chemistry, 1949, **41**, 1179.

[38] R.H. Perry and D.W. Green, Perry's chemical engineers handbook, 8th ed, New York, McGraw-Hill Professional, 2008.

[39] T.E. Daubert and R.P. Danner, Physical and thermodynamic properties of pure chemicals: Data compilation, 2nd ed, Washington DC, Taylor & Francis, 1992.

[40] S.S.E.H. Elnashaie and S.S. Elshishini, Modelling, Simulation and Optimization of Industrial Catalytic Fixed Bed Reactors, Amsterdam, Gordon and Breach, 1993.

[41] R.G. Rice and D.D. Do, Applied mathematics and modeling for chemical engineers, 2nd ed, Wiley-AIChE, 2012.

[42] J. Lee and D.H. Kim, Chemical Engineering Science, 2005, **60**, 5569.

[43] L. Gosselin, M. Tye-Gingras and F. Mathieu-Potvin, International Journal of Heat and Mass Transfer, 2009, **52**, 2169.

[44] E.G. Shopova and N.G. Vaklieva-Bancheva, Computers & Chemical Engineering, 2006, **30**, 1293.

[45] Process Economics Program Report SRI 44-A , Ammonia, 1980.